JOURNAL OF MECHANICS OF CONTINUA AND MATHEMATICAL SCIENCES
www.journalimcms.org

ISSN (Online): 2454 -7190, Vol.-20, No.-7, July (2025) pp 136-153 ISSN (Print) 0973-8975

NUMERICAL INVESTIGATION OF MWCNT/ZNO HYBRID NANOFLUID HEAT PERFORMANCE OF A COUNTER FLOW HEAT EXCHANGER

Pidaparthy Maheshbabu[1], R. Ramkumar[2], Goda Sreenivasulu Reddy[3] M. Bakkiyaraj[4], Prakash H. Jadhav[5]

[1,2] Department of Mechanical Engineering, Faculty of Engineering and Technology, Annamalai University, Tamil Nadu, India.

[1] Department of Mechanical Engineering, CMR College of Engineering & Technology, Telangana, India.

[3]Department of Mechanical Engineering, Mahatma Gandhi Institute of Technology, Hyderabad-500075, Telangana, India.

[4]Department of Mechanical Engineering, Rajalakshmi Institute of Technology, Chennai-600124, Tamil Nadu, India.

[5]Department of Mechanical Engineering, RMD Sinhgad School of Engineering, Warje, Pune-411058, Maharashtra, India.

Email: [1] maheshbabu.1045@gmail.com, [2]rramkumarhai@gmail.com, [3]gsreddy.nitk@gmail.com, [4]bakya1984@gmail.com, [5]jdvprakash@gmail.com,

Corresponding Authors: **Pidaparthy Maheshbabu**

https://doi.org/10.26782/jmcms.2025.07.00008

(Received: April 09, 2025; Revised: June 16, 2025; Accepted: July 01, 2025)

Abstract

The numerical study explores the augmentation of heat dissipation rate and efficiency of a counter flow heat exchanger (CFHEx) in the presence of (MWCNT/ZnO) hybrid nanofluids (HNF). The HNF concentration is varied from 0.01% to 0.05% in steps of 0.02%. The Reynolds number (Re) of cold fluid is varied from 2436 to 11626, while that of hot fluid, Re, is kept constant. The typical k-ε model is utilized for the numerical simulation in turbulent flow regimes. The current numerical results are compared to the literature to serve as validation purpose. From the validation study, the Nusselt (Nu) number agrees well with the numerical and experimental data of the literature, with a deviation of less than 6%. From the numerical study, it can be observed that when the concentrations of HNF the Nu number intensifies meaningfully with a rise in the Re number. For HNF concentration of 0.05%, the average increase in Nusselt number (Nu) is found to be around 41.35% and 23.13% higher than that of base fluid water and 0.01% concentration of HNF, respectively, with an adequate rise in the pressure drop. The critical performance evaluation criteria are also determined, and it is found that at higher concentrations, of hybrid nanofluid performs better than

at lower concentrations of the hybrid nanofluid. In addition, the PEC is found to be maximum at lower Re numbers, and further, it reduces with an increase in the flow Re number.

Keywords: Friction factor, Heat Exchanger, Hybrid nanofluid, Nusselt number, Performance evaluation criteria.

I. Introduction

In today's scenario, heat transfer equipment requires more effective and efficient solutions for the enhancement of heat transfer for growing industry demand and space-efficient heat transfer (HT) systems. Many efforts have been made for the enhancement of heat transfer in account of nanofluids (NF) [X]. The application of heat transfer is more important for the regulation of heat dissipation rate used in electric cars, thermal solar collectors, spacecraft, food, and chemical processing industries, as referred to [XVII]. Most of the researchers have assumed various scenarios for the augmentation of heat transfer, like baffles [VI] & [XVI], extended surfaces [XI], porous media [XX, XXI, XXII, & XXIII], and nanofluids [VII, XXXIV]. However, by accompanying the baffles, extended surfaces, and porous media leads to higher pumping power reported in [XXIV, XXVI]. However, the pressure drop can be reduced with the use of NF and HNF with the maximum possible rate of HT. Therefore, to minimize the pressure drop with the maximum possible rate of HT, the authors have decided to conduct the numerical investigations with use of HNF. The study considered sinusoidal corrugated channel influence on heat transfer (HT) and pressure drop in the turbulent flow regime, whose Re range from 6000 to 22,000, detailed in Aliabadi [I]. The corrugated channel containing nanofluid attains the highest Nu number when compared to the base fluid [XV]. The multi-objective optimization study is proposed to determine the HT and pressure drop of a twin tube heat exchanger (HEx) was investigated by Esfe et al. [XIV]. They claimed that the system's cost had dropped about 38% as compared to the best-case scenario. The literature is further extended to include different inserts' influence on pressure drop and HT. Prasad et al. [XXIX] reported that the friction factor (FF) increased 1.29 times for a nanofluid concentration of 0.03% in association with the base fluid.

Singh and Sarkar [XXXIII] recently reported that increasing the depth ratio (DR) and twist ratio (TR) of twisted tape (TT) in combination with nanofluid leads to better heat transfer at the expense of friction resistance. In addition, Nakhchi and Esfahani [XII] reported that the increase in heat transfer is found to be 48.0%, 64.3%, 86.0%, and 117.4% higher for twist ratios of 0.6, 1, 1.4, and 1.8, respectively, in comparison to a case without TT inserts. Aghayari et al. [XXX] claimed that the Nu number agument significantly and monotonically with higher and lower mass flow rates with marginal increase in the friction factor. Kumar et al. [XIX] observed that at Re = 11,000, the maximum PEC is attained to be 1.74 with constant TR and WR. Further, Nakhchi and Esfahani [XIII] studied the tube heat exchanger performance with insertion of TT inserts in the presence of NF, and they found that the HTR improves meaningfully due to better mixing of fluid at the core and near the wall of the tube heat exchanger. The PEC of tube HEx in the presence of HNF is found to be 1.068 with $\varphi = 1.8$ at flow Re = 8320 as per [XVIII]. According to recent studies of literature [III, VIII & XXXII],

suggested that the NTU and the effectiveness of HEx can be improved by using TT inserts and in combination with nanofluid.

Further, Khargotra et al. [XXV] examined the heat transmission through tube HEx and they noticed that the HTR can be improved from fluid to tube is attributed to enhanced turbulence that breaks up TBL (thermal boundary layer) at the pipe wall. Li et al. [XXXVII] examined different heat fluxes, and they noted that with increasing heat flux, the HTR increases without any significant changes in the pumping power. Also, Sudheer and Madanan [V] reported that with the insertion of TT inserts, the THP improved outstandingly due to the generation of primary vortex, which causes to thinning of TBLs by secondary formation vortices. Stalin et al. [XXVIII] claimed that low thermal properties of water could prevent any appreciable improvement in the thermal performance. Henceforth, the maximization of HTR can be achieved with the use of nanofluids without a significant increase in the pressure drop. Atul Bhattad [II] conducted an experimental study with the use of HNF (Al_2O_3/MgO) in a plate HEx, and they claimed that the HNF is superior to that of NF with a slight increase in the pumping power. Mund et al. [IV] examined the performance of tube HEx in consideration of HNF. They noted that HT enhancement increases significantly with increasing concentration of HNF, with marginal growth in pumping power. Further, Ahmed et al. [XXXVI] examined the experimental study to determine the PEC and effectiveness of HEx. For maximum addition of nanoparticles to the base fluid leads to enhanced HTC. Since higher concentration of nanoparticles in the base fluid leads to more collisions of nanoparticles with each other, it leads to an increase in HTC. However, at higher concentrations of HNF, the HTR is found to be 69% higher when compared to the base fluid. Recently, Plant et al. [XXXI] explored the thermal performance and effectiveness of CFTHEx accompanied by various concentrations of HNF with magnetic field effect. They determined that with the influence of the magnetic field and HNF, the Nu number is augmented by almost 40% when compared to the base fluid.

From the literature, many authors have performed experimental and numerical investigations of heat exchangers using NF and HNF. However, very few studies have been conducted to determine the performance of a heat exchanger with the use of MWCNT/ZnO HNF. Therefore, the present study mainly focused on assessing the performance of a heat exchanger using MWCNT/ZnO HNF for the various thermal engineering applications. The important applications include car radiators, solar heaters, and food processing industries.

Research Significance

As far as we are aware, there aren't many published works using hybrid nanofluids in a CFHEx. Henceforth, the focus of the present research will be on the application of vehicle exhaust treatment, vehicle radiators, and solar collectors. The innovation of the research is the evaluation of the work of CFHEx with a hybrid nanofluid. Microparticles that have been modified on the outside and nanoparticles that are compatible with the base fluid are responsible for the increased thermal conductivity provided by HNF. Therefore, the authors have carried out three (0.01%, 0.03% and 0.05%) different percentages of hybrid nanofluid. The employment of HNF blends with cold fluid that flows inside CFHEx.

II. Numerical domain of counter flow heat exchanger (CFHEx)

Commercial software ANSYS FLUENT 19.2 is used for the numerical simulation as per refs. [XXVII, IX]. The shell side walls are assigned to adiabatic wall conditions. For numerical simulation, the flow is considered to be steady state, homogeneous, and single phase. For better accuracy, the equations *k-ε* turbulence model are utilized for the numerical simulation [XXXIV] & [IX]. The Reynolds number varied from 2436 to 11626 depending on the hydraulic diameter of the tube. The shell side of the HEx, Re number (8,322) is maintained constant. The tetrahedral mesh is used for the numerical simulations. The skewness of the mesh is found to be less than 0.25, and the orthogonal quality of the mesh is observed to be greater than 0.75. The convergence criterion is set as 10^{-5} for the continuity and momentum equations and 10^{-6} for the energy equation [XXXIV] & [IX]. The specification of CFHEx is reported in Table 1. The numerical geometry and mesh model of CFHEx are presented in Figure 1 and Figure 2(a) and (b), respectively. For the numerical computations, thermo-physical properties of MWCNT/ZnO considered for the numerical simulation are presented in Table 2.

Table 1: The CFHEx specification refs. [11]

CFHEx	value
Tube length (mm)	2600
Entry temp. of hot fluid	60^0 C
Entry temp. of cold fluid	30^0 C
Outer tube OD (mm)	63
Outer tube ID (mm)	60
Inside tube OD (mm)	19
Inside tube ID (mm)	17
Outer tube	Mild steel
Inner tube	Copper

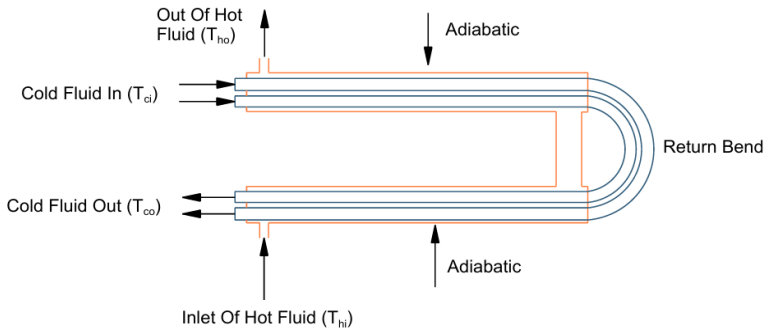

Fig. 1. Line diagram of counterflow heat exchanger.

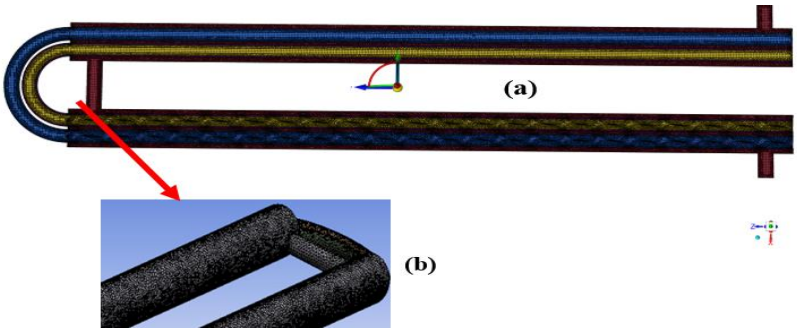

Fig 2. Numerical domain and mesh model of counterflow heat exchanger

Table 2. Properties of MWCNT/ZnO HNF

S. No.	Concentration (%)	Temperature (°C)	Density (Kg/m^3)	Viscosity (N-s/m^2)	Sp. Heat (J/kg K)	Thermal conductivity (W/m K)
1	0.01	30	1008	0.00193	4183	0.982
		40	1003	0.00167	4182	1.042
		50	998	0.00132	4181	1.121
		60	990	0.00113	4152	1.326
2	0.03	30	1053	0.00186	3952	1.094
		40	1042	0.00156	3986	1.254
		50	1036	0.00074	3986	1.319
		60	1026	0.00064	4008	1.502
3	0.05	30	1071	0.00176	3888	1.27
		40	1069	0.00144	3879	1.295
		50	1060	0.00094	3893	1.424
		60	1059	0.00082	3881	1.564

The governing equations of continuity, momentum, and energy equations are adopted for the numerical simulations as per refs. [XXXIV] & [IX]. For the numerical simulation, the fluid is considered to be steady state, single phase, and homogeneous.

Contunuity equatuion,

$$\frac{\partial(\rho u_i)}{\partial x_i} = 0 \tag{1}$$

Momentum equation,

$$\frac{\partial(\rho u_i u_j)}{\partial x_j} = -\frac{P}{x_i} + \frac{\partial}{\partial x_i}\left[\frac{\partial(u_i)}{\partial x_j} - \rho u_i' u_j'\right] \tag{2}$$

Energy equation,

$$\frac{\partial}{\partial x_i}(\rho T) + \frac{\partial}{\partial x_i}(\rho u_i T) = -\frac{\partial}{\partial x_i}\left[\frac{k}{c_p}\frac{\partial T}{\partial x_i}\right] \tag{3}$$

Where,

$$u_j \frac{\partial k}{\partial x_j} = v_T \left[\left(\frac{\partial u_i}{\partial x_j} + \frac{\partial u_j}{\partial x_i}\right)\frac{\partial u_i}{\partial x_j}\right] - \varepsilon + \frac{\partial}{\partial x_j}\left[\left(v + \frac{v_T}{\sigma_k}\right)\frac{\partial k}{\partial x_j}\right] \quad (4)$$

$$u_J \frac{\partial \varepsilon}{\partial x_j} = C_{\varepsilon 1} v_T \left[\left(\frac{\partial u_i}{\partial x_j} + \frac{\partial u_J}{\partial x_i}\right)\frac{\partial u_i}{\partial x_j}\right] + C_{\varepsilon 2}\frac{\varepsilon^2}{k} + \frac{\partial}{\partial x_j}\left[\left(v + \frac{v_T}{\sigma_\varepsilon}\right)\frac{\partial k}{\partial x_j}\right] \quad (5)$$

Thermal properties of nanofluid are evaluated as per [II, IV].

$$\rho_{Hyb.nf} = (1-\varphi)\rho_{bf} + \rho_p \quad (6)$$

$$Cp_{Hyb.nf} = \frac{(1-\varphi)(\rho Cp)_{bf} + \varphi(\rho Cp)_p}{\rho_{Hyb.nf}} \quad (7)$$

Where $\rho_{Hyb.nf}$ represents density and $Cp_{Hyb.nf}$ represents specific heat. The dynamic viscosity of the hybrid nanofluid is computed in refs. [II, IV].

$$\mu_{Hyb.nf} = (1 + 2.5\varphi)\mu_{bf} \quad (8)$$

Actual thermal conductivity is determined using relation [II, IV].

$$k_{Hyb.nf} = \frac{k_p + 2k_{bf} - 2(k_{bf} - k_p)\varphi}{k_p + 2k_{bf} + 2(k_{bf} - k_p)\varphi} \quad (9)$$

The heat transfer between the cold and hot fluid of the heat exchanger is calculated with the help of the Eqs. (10) and (22).

$$Q_h = \dot{m} C_{P,h}(T_{h,i} - T_{h,o}) \quad (10)$$

$$Q_c = \dot{m} C_{P,c}(T_{c,o} - T_{c,i}) \quad (12)$$

The mean HT between the cold and hot fluid is evaluated using Eqs (13) and (14).

$$Q_{avg} = \frac{Q_c + Q_h}{2} \quad (13)$$

$$Q_{avg} = U_i A_i \Delta T_{LMTD} \quad (14)$$

Where, A_i, ΔT_{LMTD} denotes the area of the heat exchanger and logarithmic mean temperature difference computed using Eqs. (15) & 1(6).

$$A_i = \pi d_i L \quad (15)$$

$$\Delta T_{LMTD} = \frac{(\Delta T_1 - \Delta T_2)}{ln\left(\frac{\Delta T_1}{\Delta T_2}\right)} \quad (16)$$

Where, ΔT_1 and ΔT_2 represents inlet temperature difference & outlet temperature difference among hot and cold fluids, and are determined using Eq. (17).

$$\Delta T_1 = (T_{h,i} - T_{c,o})$$
$$\Delta T_2 = (T_{h,o} - T_{c,i}) \quad (17)$$

Boundary conditions (BC's)

The hot fluid Re number (Re = 8,322) is maintained constant while that of the cold fluid Re number changes from 2,436 to 11,626. The cold fluid's input temperature is maintained at 30ºC, while the hot fluid temperature is maintained constant at 60ºC. Because of the solid surface, no no-slip boundary condition is used at the walls. Table 3 presents the specifics of the boundary conditions.

Table 3: BC's adopted for the numerical simulations

Boundary condition	Annulus	Tube
Reynolds number (Re)	8,322	2,436 to 11,626
Temperature	60º C	30º C
Walls of shell & tube	Adiabatic	Diathermic
Walls	No slip	No slip

III. Results and Discussions

III.i. Grid independence study

Figure 3 presents the grid size test for various numbers of cells versus pressure drop changes. The grid study is accomplished for a high Re (Re = 11625) number. From the figure, it is observed that the grid size of 3224789 is found to be marginally similar in pressure drop compared to a higher number of grid sizes. Therefore, for computing minimal CPU time, the grid size of 3224789 is considered for further computations.

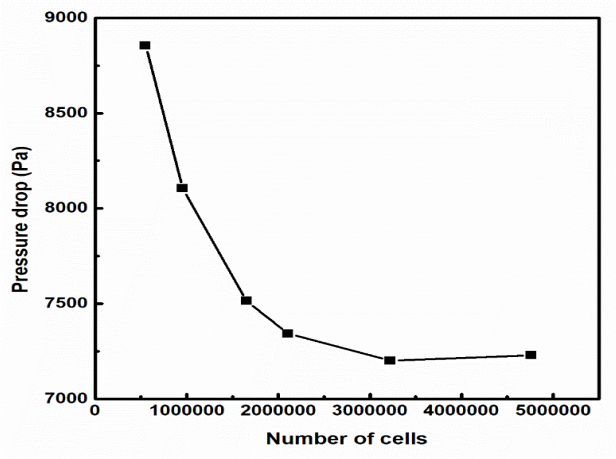

Fig. 3. Numerical domain and mesh model of counterflow heat exchanger

III.ii. Validation study

The validation study is performed to affirm the current approach of the numerical simulation. Figure 4 explores the comparative results of the Nu number with experimental and numerical studies in the available literature of [XXXIV]. From the results, it is observed that the results of the Nu number follow a similar tendency compared to the literature [XXXIV]. However, the discrepancy between the present study compared to experimental and numerical results is found to be less than 5.7% and which is well acceptable in the acceptable range.

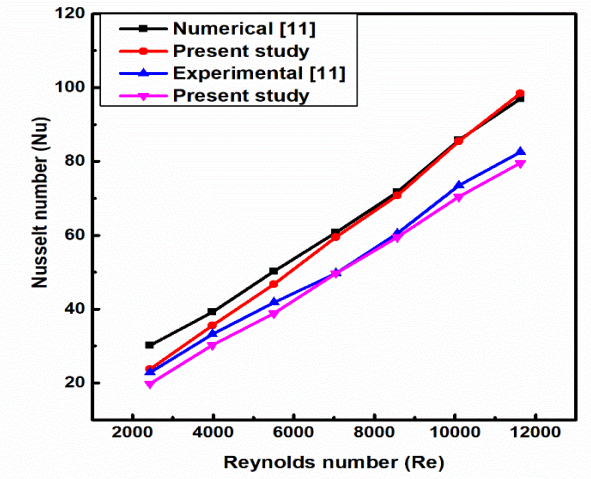

Fig. 4. Numerical domain and mesh model of counterflow heat exchanger

III.iii. Heat transfer coefficient (HTC)

Figure 5 presents HTC versus Reynolds number (Re) for the base fluid and various concentrations of MWCNT/ZnO HNF. The HTC increases significantly with increasing Re number as well as increasing the concentrations of HNF. Since, maximum values of Re number growth, the turbulent intensity causes mixing of the fluid and hence enhancement in the HTC. Also, the momentum of the fluid increases at higher values of Re number. Additionally, for higher values of Re number, the hybrid nanofluid is forced to flow, leading to an enhancement in the HTC. From the CFD simulation study, the backflow and flow separation phenomenon at the bend section of the numerical domain. However, at 0.05% concentration of hybrid nanofluid, the mean HTC enhancement is observed to be 58.96% and 23.04% greater compared to the base fluid and 0.01% concentration of hybrid nanofluids, respectively. This is due to that there is a significant increase in thermal conductivity of the hybrid nanofluid compared to the base fluid. A similar tendency was observed in the literature [XXXIV] & [IX].

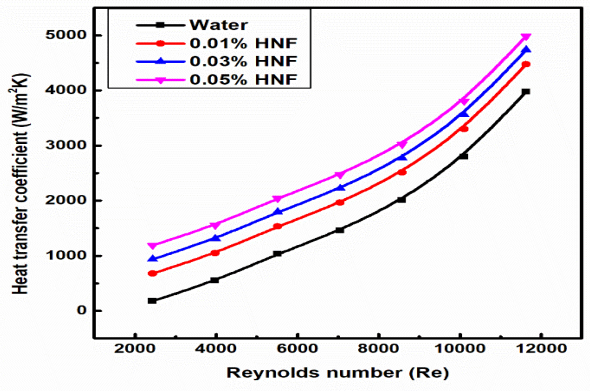

Fig. 5. HTC vs. Re for base fluid and hybrid nanofluid

III.iv. Overall heat transfer coefficient (OHTC, U_i)

The OHTC is often denoted by U_i, is a crucial parameter in thermal engineering with significant implications across various fields. It quantifies how readily heat is transferred through a combination of different materials and fluid layers, considering conduction and convection heat transfer. The OHTC was computed using relations (18) and (19).

$$\frac{1}{U_i}=\frac{1}{h_i}+B \tag{18}$$

Where, h_i is HTC, and B is constant and which is computed with account of the Wilson chart according to ref. [XXXIV] & [VIII].
The U_i is calculated using Eq. (19).

$$U_i=\frac{Q_{avg}}{A_i\,\Delta T_{LMTD}} \tag{19}$$

Figure 6 presents OHTC against Re for various concentrations of HNF, base fluid water, and CeO_2 NF with literature [XXXIV]. The mean OHTC presents the greatest and least values for 0.05% concentrations of HNF & base fluid, respectively. For a fixed temperature of hot fluid, the average heat dissipation rate increases amongst hot & cold fluids as a result of an increase in OHTC. However, at higher concentrations of hybrid nanofluid, augment thermal conductivity of the fluid is augmented. Therefore, the amount of heat absorption rate between and hot and cold fluid is more than base fluid, as an increase in the OHTC. From the study, maximum concentrations (i.e., 0.05%) of hybrid nanofluid are augmented by 45.01% relative to the base fluid. Henceforth, higher concentrations of hybrid nanofluid are more promising for the augmentation of OHTC. In addition, the OHTC results of the present study are also compared with the results of NF available in the literature of [XXXIV]. From the study, the results of OHTC with the use of HNF were much higher when compared to the results of NF in the literature [XXXIV]. For 0.01%, 0.03% and 0.05% concentrations of HNF, the OHTC augments 15.72%, 16.16% and 20.88% more relatively to 0.10%, 0.20% and 0.30% concentrations of NF, respectively reported in [XXXIV] in the range of flow Re is simulated.

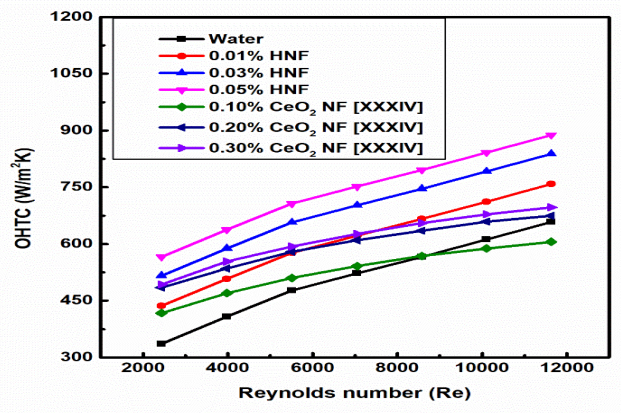

Fig. 6. OHTC vs. Re for base fluid and hybrid nanofluid

III.v. Nusselt number (Nu)

The Nu number is evaluated using the Eq. (20). The Nusselt number signifies the ratio of convection heat transfer through the fluid to the conduction heat transfer through the same fluid.

$$\mathrm{Nu} = \frac{h_i\, d_i}{K_f} \tag{20}$$

Figure 7 explores the computed numerical results of Nu for the base fluid & various concentrations of HNF with the flow Re number. Nevertheless, in comparison to base fluid & 0.01% concentrations of HNF, the 0.05% concentrations of HNF present the utmost Nu number among the Re numbers simulated. This could be because the effective thermal conductivity of MWCNT/ZnO nanofluid increases with increasing concentration of MWCNT/ZnO nanoparticles and allowing the fluid to absorb maximum heat from the heating fluid flowing beneath the shell side of a counter flow heat exchanger (CFHEs). Higher Re numbers cause proper mixing of the fluid, which tends to increase HTC and Nu numbers. For higher concentrations of HNF, the average Nu number increases by 41.07% and 23.43% related to the base fluid and 0.01% concentration of HNF, respectively. Further, the numerical results of the Nu number are compared with the literature of [XXXIV], due to the author of [XXXIV] has considered for same domain and the same Re number for their experimental and numerical investigations. The presence of 0.01%, 0.03% and 0.05% concentrations of HNF, the augmentation of Nu number is obtained to be 14.28%, 16.13% and 16.78% higher when compared to literature [XXXIV] with 0.10%, 0.20% and 0.30% concentrations of CeO_2 nanofluids (NF).

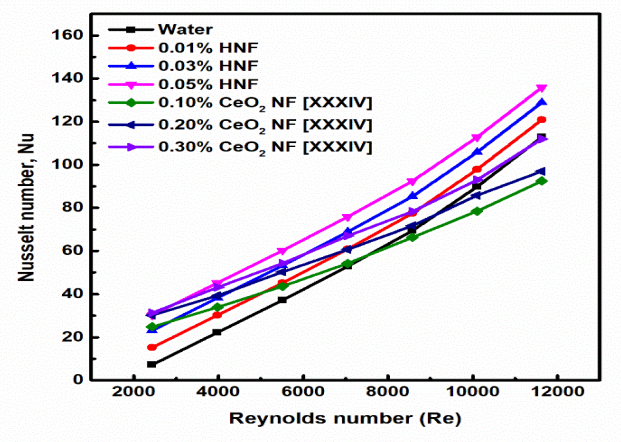

Fig. 7. Nu vs. Re for base fluid and hybrid nanofluid.

III.vi. Pressure drop (Pd)

Figure 8 shows the comparative study of Pd for different concentrations of HNF & base fluid with respect to the flow Re number. The result reveals that both an increase in Re number and HNF concentration cause an increase in pressure drop. However, at lower Re numbers, the rise in Pd is considerably less than the higher values of Re number. This is because at lower Re numbers, fluid flows at a lesser intensity, leading to lower pressure drops. Further, increasing the concentration of HNF in the base fluid water leads to an increase in pressure drop due to an increase in the viscosity of the fluid. In contrast to the base fluid water, the increase in pressure drop is much less than that of higher nanoparticle concentrations. This is due to the possibility of the flow separation phenomena at the pipe bend section, which raises the pressure due to backflow. Additionally, there may be an uneven flow distribution inside the twin-tube counterflow heat exchanger, which would result in a greater pressure drop. Conversely, the pressure drop increases with increasing concentrations of HNF. Because a higher concentration of HNF results in a higher viscosity, which may cause to increase in the pressure drop. To easily differentiate the pressure variation, contours are presented for three different Re numbers, as shown in Figure 9. It is noted from the figure that the pressure drops significantly at higher maximum flow Re numbers, which is observed in the pressure contour plots. Furthermore, the result of pressure drop accompanied by HNF is compared with the CeO_2 nanofluid (NF) reported in the literature [XXXIV]. From the observation, it is noticed that the HNF pressure drop result presents the highest pressure drop when compared to the CeO_2 nanofluid reported in Ref. [XXXIV]. This is because the viscosity of HNF is higher than that of CeO_2 NF. That is why the pressure developed is more with the use of HNF.

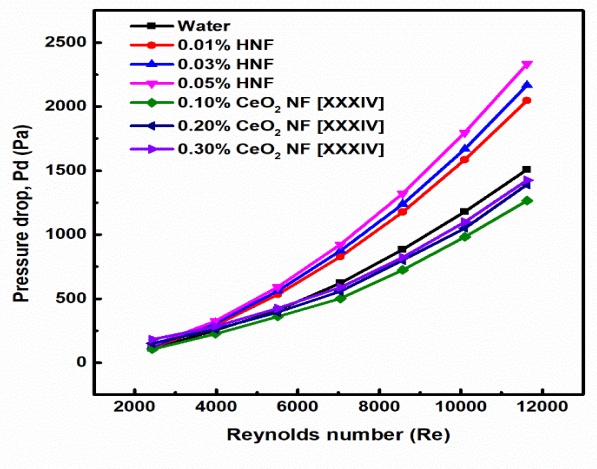

Fig. 8. Pd vs. Re changes for base fluid and hybrid nanofluid

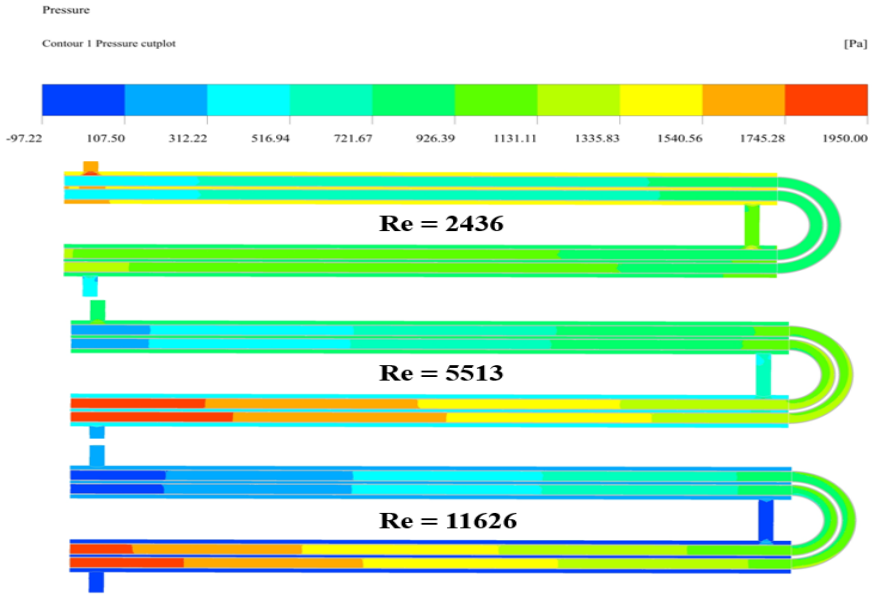

Fig. 9. Pressure contours for different Re numbers.

III.vii. Friction factor (FF)

The FF is a dimensionless quantity that quantifies to measures the resistance of fluid through the heat exchanger. The FF was computed using the Eq. (21) as per [VIII].

$$f = \frac{\Delta P}{\frac{L}{d_i}\left(\frac{\rho V^2}{2}\right)} \qquad (21)$$

Figure 10 presents the FF of CFHEx and which increases with increasing concentration of HNF and reduces with an increase in the Re number. Since, addition of nanoparticles

to the base fluid leads to an increase in the viscosity and thereby an increase in the pumping power as a result increase in the flow resistance. Friction resistance may also increase due to incorrect dispersion of nanoparticles in the base fluid. For all fluids taken into consideration for this investigation, the friction factor is larger for lower Reynolds numbers. Nonetheless, under the conditions of higher mass flow rates, the friction factor decreases. At 0.05% concentrations of HNF, the friction resistance is found to be maximum when compared to 0.03% and 0.01% concentrations of HNF & base fluid, respectively.

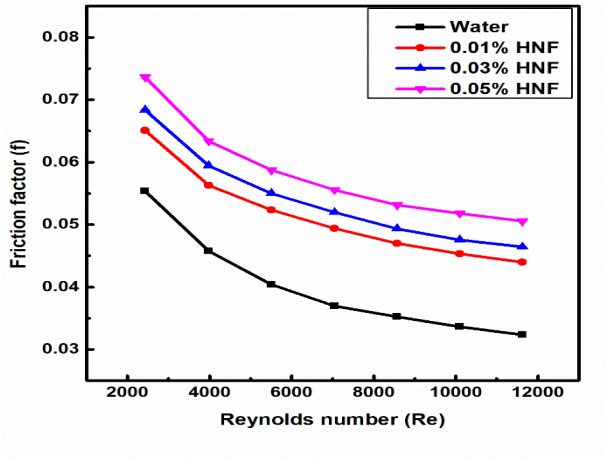

Fig. 10. FF vs. Re for various fluids

III.viii. Performance evaluation criteria (PEC)

The PEC indicates the CFHEx performance. The PEC is the ratio of the heat transfer enhancement to one-third of the pumping power. The PEC measures the performance of the heat exchanger under the influence of three different concentrations of HNF. The PEC is evaluated with the Eq. (22) as per [XI, VIII].

$$PEC = \frac{\left(\frac{Nu_{Hyb.nf}}{Nu_{bf}}\right)}{\left(\frac{f_{Hyb.nf}}{f_{bf}}\right)^{1/3}} \tag{22}$$

Figure 11 shows the outcomes of PEC against Re number for various concentrations of MWCNT/ZnO HNF & base fluid water. Figure 11 shows that, for all fluid concentrations taken into consideration, the PEC is found to be more than 1. But according to the numerical study, the PEC for 0.05% HNF presents the highest PEC at lower Re numbers and decreases sharply with the growing Re number. Furthermore, the PEC was found to be significantly higher for higher concentrations of nanofluid than the lower concentrations of nanofluid. However, for a 0.05% concentration of HNF, the average increase in PEC is found to be 40.03% more than the lower concentration of HNF in the range of Re that is simulated.

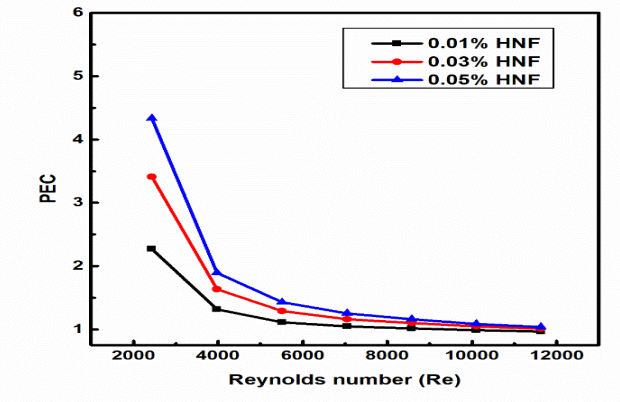

Fig. 11. PEC vs. Re for nanofluid concentrations

IV. Conclusion

The objective of the study is to critically examine CFHEx along with various concentrations of hybrid nanofluid. The Re number of fluid changes from 2436 to 11626 and HNF concentration changes from 0.01% to 0.05% in steps of 0.02%. The numerical simulations are performed using ANSYS Fluent. The investigations yielded the following important findings, which are listed below:

I. From the study, 0.05% concentration of MWCNT/ZnO HNF, the average augmentation in HTC is found to be 58.96% higher in comparison to the base fluid water, within the range of Re that is simulated.

II. The HTC increases significantly with increasing concentrations of HNF as well as the flow Re number. In addition, maximum concentrations of HNF the the OHTC are found to be 45.01% greater than that of the base fluid water.

III. The Nu number increases considerably with increasing Re number in the range of Re that is simulated. However, the augmentation of average Nu number by almost 41.07.38% and 23.43% higher than that of the base fluid water and 0.01% concentration of MWCNT/ZnO HNF.

IV. The PEC is found to be significantly higher at lower values of Re number, while it diminishes with an increase in Re number. However, the PEC is found to be greater than 1 for all concentrations of nanofluid in the range of Re investigated.

V. From the study, the HT results showed a significant enhancement with the use of HNF, with a considerable increase in friction resistance when compared to the results of nanofluids reported in literature [XXXIV].

V. Acknowledgements

I would like to thank the management of Annamalai University and CMR College of Engineering & Technology for the facilities they provide and their support.

Conflict of Interest:

There was no relevant conflict of interest regarding this paper.

References

I. A. Beheshti, M. K .Moraveji, M. Hejazian. : 'Comparative numerical study of nanofluid heat transfer through an annular channel'. *Numerical Heat Transfer, Part A: Applications*. Vol. 67, pp. 100-117, 2015. 10.1080/10407782.2014.894359.

II. A. Bhattad. : 'Experimental investigation of Al_2O_3-MgO hot hybrid nanofluid in a plate heat exchanger'. *Heat Transfer*. Vol. 49, pp. 1-11, 2020. 10.1002/htj.21724

III. A. Kumar, S. Sharma, S. Kumar, R. Maithani. : 'Thermohydraulic analysis of twisted tape inserts with SiO_2/H_2O nanofluid in heat exchanger'. *Australian Journal of Mechanical Engineering*. Vol. 00, pp. 1-14, 2021. 10.1080/14484846.2021.1960672.

IV. A. Mund, B. Pattanayak, J. S. Jayakumar, K. Parashar, S. K. S. Parashar. : 'Experimental and Numerical Study of Heat Transfer in Double-Pipe Heat Water Nanofluid'. *Advances in Fluid and Thermal Engineering.* Vol. 1, pp. 531-540, 2019. 10.1007/978-981-13-6416-7.

V. A. P. Sudheer, U. Madanan. : 'Numerical investigation into heat transfer augmentation in a square minichannel heat sink using butterfly inserts'. *Thermal Science and Engineering Progress.* Vol. 36, pp. 101522, 2022. 10.1016/j.tsep.2022.101522.

VI. G. Huminic, A. Huminic. : 'Application of nanofluids in heat exchangers: A review'. *Renewable and Sustainable Energy Reviews.* Vol. 16, pp. 5625-5638, 2012. 10.1016/j.rser.2012.05.023.

VII. G. Narendran, P. H. Jadhav, N. Gnanasekaran. : 'A smart and sustainable energy approach by performing multi-objective optimization in a minichannel heat sink for waste heat recovery applications'. *Sustainable Energy Technologies and Assessments*. Vol. 60, pp. 103447, 2023. 10.1016/j.seta.2023.103447.

VIII. G. Narendran, P. H. Jadhav, N. Gnanasekaran. : 'Numerical analysis of thermo hydro-dynamics behavior of solar flat plate collector with square and V-cut twisted tape inserts'. *Numerical Heat Transfer, Part A: Applications*. Vol. 84, pp. 1-25, 2023. 10.1080/10407782.2023.2294043.

IX. G. S. Reddy, R. Kalaivanan, R. U. Kumar, P. H. Jadhav. : 'Influence of W-cut twisted tape inserts on heat transfer characteristics of a counter flow heat exchanger using CeO_2 nanofluid - an experimental and numerical investigations'. *Numerical Heat Transfer, Part A: Applications*. Vol. 85, pp. 1-21, 2024. 10.1080/10407782.2024.2359060.

X. H. Maddah, M. Alizadeh, N. Ghasemi, S. R. Wan Alwi. : 'Experimental study of Al_2O_3/water nanofluid turbulent heat transfer enhancement in the horizontal double pipes fitted with modified twisted tapes'. *International Journal of Heat and Mass Transfer*. Vol. 78, pp. 1042-1054, 2014. 10.1016/j.ijheatmasstransfer.2014.07.059.

XI. K. Aroonrat, C. Jumpholkul, R. Leelaprachakul, A. S. Dalkilic, O. Mahian, S. Wongwises. : 'Heat transfer and single-phase flow in internally grooved tubes'. *International Communications in Heat and Mass Transfer*. Vol. 42, pp. 62-68, 2013. 10.1016/j.icheatmasstransfer.2012.12.001.

XII. M. E. Nakhchi, J. A. Esfahani. : 'Numerical investigation of rectangular-cut twisted tape insert on performance improvement of heat exchangers'. *International Journal of Thermal Sciences.* Vol. 138, pp. 75-83, 2019. 10.1016/j.ijthermalsci.2018.12.039.

XIII. M. E. Nakhchi, J. A. Esfahani. : 'Performance intensification of turbulent flow through heat exchanger tube using double V-cut twisted tape inserts'. *Chemical Engineering & Processing: Process Intensification*. Vol. 141, pp. 107533, 2019. 10.1016/j.cep.2019.107533.

XIV. M. Hemmat Esfe, H. Hajmohammad, D. Toghraie, H. Rostamian, O. Mahian, S. Wongwises. : 'Multi-objective optimization of nanofluid flow in double tube heat exchangers for applications in energy systems'. *Energy*. Vol. 137, pp. 160-171, 2017. 10.1016/j.energy.2017.06.104.

XV. M. Khoshvaght-aliabadi, A. Feizabadi. : 'Compound heat transfer enhancement of helical channel with corrugated wall structure'. *International Journal of Heat and Mass Transfer*. Vol. 146, pp. 118858, 2020. 10.1016/j.ijheatmasstransfer.2019.118858.

XVI. M. M.Elias, I. M. Shahrul, I. M. Mahbubul, R. Saidur, N. A. Rahim. : 'Effect of different nanoparticle shapes on shell and tube heat exchanger using different baffle angles and operated with nanofluid'. *International Journal of Heat and Mass Transfer*. Vol. 70, pp. 289-297, 2014. 10.1016/j.ijheatmasstransfer.2013.11.018.

XVII. M. M. Rahman, S. Saha, S. Mojumder, A. G. Naim, R. Saidur, T. A. Ibrahim. : 'Effect of Sine-Squared Thermal Boundary Condition on Augmentation of Heat Transfer in a Triangular Solar Collector Filled with Different Nanofluids'. *Numerical Heat Transfer, Part B: Fundamentals.* Vol. 68, pp. 37-41, 2015. 10.1080/10407790.2014.992058.

XVIII. N. F. A. Hamza, S. Aljabair. : 'Evaluation of thermal performance factor by hybrid nanofluid and twisted tape inserts in heat exchanger'. Heliyon. Vol. 8, pp. e11950, 2022. 10.1016/j.heliyon.2022.e11950.

XIX. N. T. R. Kumar, P. Bhramara, A. Kirubeil, L. S. Sundar, M. K. Singh, A. C. M. Sousa. : 'Effect of twisted tape inserts on heat transfer, friction factor of Fe_3O_4 nanofluids flow in a double pipe U-bend heat exchanger'. *International Communications in Heat and Mass Transfer.* Vol. 93, pp. 53-62, 2018. 10.1016/j.icheatmasstransfer.2018.03.020.

XX. P. H. Jadhav, N. Gnanasekaran. : 'Optimum design of heat exchanging device for efficient heat absorption using high porosity metal foams'. *International Communications in Heat and Mass Transfer*. Vol. 126, pp. 105475, 2021. 10.1016/j.icheatmasstransfer.2021.105475.

XXI. P. H. Jadhav, N. Gnanasekaran, D. A. Perumal, M. Mobedi. : 'Performance evaluation of partially filled high porosity metal foam configurations in a pipe'. *Applied Thermal Engineering*. Vol. 194, pp. 117081, 2021. 10.1016/j.applthermaleng.2021.117081.

XXII. P. H. Jadhav, N. Gnanasekaran, M. Mobedi. : 'Analysis of functionally graded metal foams for the accomplishment of heat transfer enhancement under partially filled condition in a heat exchanger'. *Energy*. Vol. 263, pp. 125691, 2023. 10.1016/j.energy.2022.125691.

XXIII. P. H. Jadhav, G. Nagarajan, D. A. Perumal. : 'Conjugate heat transfer study comprising the effect of thermal conductivity and irreversibility in a pipe filled with metallic foams'. *Heat and Mass Transfer*. Vol. 57, pp. 911-930, 2020. 10.1007/s00231-020-03000-x.

XXIV. P. H .Jadhav, N. Gnanasekaran, D. A. Perumal. : 'Numerical consideration of LTNE and Darcy extended Forchheimer models for the analysis of forced convection in a horizontal pipe in the presence of metal foam'. *Journal of Heat Transfer*. Vol. 143, pp. 1-16, 2021. 10.1115/1.4048622.

XXV. P. H. Jadhav, T. G, N. Gnanasekaran, M. Mobedi. :' Performance score based mulri-objective optimization for thermal dasign of partially filled high porosity metal foam pipes under forced convection'. *International Journal of Heat and Mass Transfer*. Vol. 182, pp. 121911, 2022. 10.1016/j.ijheatmasstransfer.2021.121911.

XXVI. P. H. Jadhav, N. Gnanasekaran, D. A. Perumal. : 'Thermodynamic analysis of entropy generation in a horizontal pipe filled with high porosity metal foams'. *Materials Today: Proceedings*. Vol. 51, pp. 1598 – 1603, 2022. 10.1016/j.matpr.2021.10.451.

XXVII. P. H. Jadhav, B. Kotresha, N. Gnanasekaran, D. Arumuga Perumal. : 'Forced Convection Analysis in a Horizontal Pipe in the Presence of Aluminium Metal Foam-A Numerical Study'. *Springer Singapore*. pp. 1-15, 2021. 10.1007/978-981-16-0698-4_53.

XXVIII. P. M. Joseph, S. T. V.Arjunan, M. M. M. N. Sadanandam. : 'Experimental and theoretical investigation on the effects of lower concentration CeO2/water nanofluid in flat-plate solar collector'. *Journal of Thermal Analysis and Calorimetry*. Vol. 131, pp. 1-15, 2017. 10.1007/s10973-017-6865-4.

XXIX. P. V. D. Prasad, A. V. S. S. K. S. Gupta, K. Deepak. : 'Investigation of Trapezoidal-Cut Twisted Tape Insert in a Double Pipe U-Tube Heat Exchanger using Al2O3 / Water Nanofluid'. Procedia Materials Science. Vol. 10, pp. 50-63, 2015. 10.1016/j.mspro.2015.06.025.

XXX. R. Aghayari, H. Maddah, S. M. Pourkiaei, M. H. Ahmadi, L. Chen, M. Ghazvini. : 'Theoretical and experimental studies of heat transfer in a double-pipe heat exchanger equipped with twisted tape and nanofluid'. *The European Physical Journal Plus*. Vol. 135, pp. 123, 2020. 10.1140/epjp/s13360-020-00252-8.

XXXI. R. Dakota, P. Gregory, K. H. Stefania, I. M. Ziad. : 'Experimental and numerical investigation of heat enhancement using a hybrid nanofluid of copper oxide / alumina nanoparticles in water'. *Journal of Thermal Analysis and Calorimetry*. Vol. 143, pp. 1-15, 2020. 10.1007/s10973-020-09639-2.

XXXII. R. Khargotra, R. Kumar, R. Nadda, S. Dhingra, T. Alam. : 'A review of different twisted tape configurations used in heat exchanger and their impact on thermal performance of the system'. *Heliyon*. Vol. 9, pp. e16390, 2023. 10.1016/j.heliyon.2023.e16390.

XXXIII. S. Kr, S. Jahar. : 'Improving hydrothermal performance of double-tube heat exchanger with modified twisted tape inserts using hybrid nanofluid'. *Journal of Thermal Analysis and Calorimetry*. Vol. 143, pp. 1-15, 2020. 10.1007/s10973-020-09380-w.

XXXIV. S. R. Goda, R. Kalaivanan, R. U. Kumar, P. H. Jadhav. : 'Experimental and numerical investigation of thermo-hydrodynamic performance of twin tube counter flow heat exchanger using cerium oxide nanofluid'. *Numerical Heat Transfer, Part A: Applications*. Vol. 84, pp. 1-19, 2023. 10.1080/10407782.2023.2268831.

XXXV. T. S. Athith, G. Trilok, P. H. Jadhav, N. Gnanasekarn. : 'Heat transfer optimization using genetic algorithm and artificial neural network in a heat exchanger with partially filled different high porosity metal foam. Material Toady: Proceedings. Vol. 51, pp. 1642-1648, 2022. 10.1016/j.matpr.2021.11.248.

XXXVI. W. Ahmed, S. N. K. Z. Z. Chowdhury, M. R. B. J. Naveed, A. M. A. Mujtaba. : 'Experimental investigation of convective heat transfer growth on ZnO@TiO_2/DW binary composites / hybrid nanofluids in a circular heat exchanger'. *Journal of Thermal Analysis and Calorimetry*. Vol. 143, pp. 1-15, 2020. 10.1007/s10973-020-09363-x.

XXXVII. W. Li, Z. Yu, Y. Wang, Y. Li. : 'Heat transfer enhancement of twisted tape inserts in supercritical carbon dioxide flow conditions based on CFD and vortex kinematics'. *Thermal Science and Engineering Progress*. Vol. 31, pp. 101285, 2022. 10.1016/j.tsep.2022.101285.